

Extremely fine pearlite by continuous cooling transformation

K.M. Wu^{a,b} and H.K.D.H. Bhadeshia^{b,*}

^aInternational Research Institute for Steel Technology, Wuhan University of Science and Technology, Wuhan 430081, China

^bMaterials Science and Metallurgy, University of Cambridge, Cambridge CB2 3QZ, UK

Received 6 January 2012; revised 17 March 2012; accepted 17 March 2012

Available online 24 March 2012

An extremely fine, fully pearlitic structure with an interlamellar spacing of 30–50 nm has been obtained during continuous cooling transformation at a rate as low as $0.1\text{ }^{\circ}\text{C s}^{-1}$, of the steel that is normally used to produce nanostructured bainite. The solutes cobalt and aluminium have been added to accelerate the rate of reaction and reduce the interlamellar spacing by increasing the free energy of transformation. The range of cooling rates over which the fully pearlitic state can be achieved is characterized.

© 2012 Acta Materialia Inc. Published by Elsevier Ltd. All rights reserved.

Keywords: Nanostructured pearlite; Continuous cooling transformation; Strong steel; Alloy design

A new range of steels has been developed in which extremely fine plates of bainite can be obtained by isothermal transformation at low homologous temperatures in very large samples [1]; the material is now commercialized and the subject has recently been reviewed [2]. The alloys typically have a hypereutectoid composition Fe–1C–1.5Si–1.9Mn–1.3Cr–0.25Mo wt.%. During the course of experiments on the transformation of austenite under the influence of a 30 tesla magnetic field, it was discovered that the continuous cooling transformation of austenite at $1\text{ }^{\circ}\text{C s}^{-1}$ resulted in the development of pearlite with an interlamellar spacing of just 50–100 nm, whereas the pearlite was not present in the absence of the field [3,4]. Such fine pearlite, obtained using a simple heat treatment, has technological potential, but the use of strong magnetic fields is prohibitively expensive and possibly impractical. Such fine spacings have previously been achieved in very-high-carbon steels containing 1.5–1.8C wt.%, but the microstructures obtained contained significant quantities of proeutectoid cementite. Similar spacings have been reported for plastically deformed pearlite [5], but the purpose here is to achieve interlamellar refinement by phase transformation.

The reason why a magnetic field stimulates the formation of pearlite is the increase in the driving force for transformation from paramagnetic austenite into ferromagnetic ferrite and cementite. The purpose of the work presented here was to see whether the fine pearlite could be obtained by enhancing the driving

force using alloying elements rather than an externally applied magnetic field.

Cobalt has long been known to increase the driving force for pearlite [6], and cobalt and aluminium increase the driving force for the formation of ferrite [7]. This characteristic of the two solutes has also been verified in the types of steels considered here [8]. It is these latter alloys, designed originally for accelerated bainitic transformation, which inspired the alloy design in the present work, where we wished to investigate the formation of pearlite during continuous cooling. Larger concentrations of aluminium and cobalt are used compared with the earlier research [8]; the compositions are listed in Table 1. Alloy 1 contains Co and Al and Alloy 2 does not. Samples were cut and then homogenized at $1200\text{ }^{\circ}\text{C}$ for 48 h in a vacuum furnace. They were then left in the furnace to cool down to room temperature over a period of 24 h to obtain a coarse and soft fully pearlitic microstructure, which can be readily machined into cylindrical samples, 8 and 12 mm long.

Continuous cooling transformation experiments were performed on a Thermecmaster thermomechanical simulator. Samples were heated at a rate of $10\text{ }^{\circ}\text{C s}^{-1}$ and held at $1000\text{ }^{\circ}\text{C}$ for 10 min for austenization prior to transformation. The samples were then continuously cooled to room temperature at a cooling rate ranging from 0.02 to $2\text{ }^{\circ}\text{C s}^{-1}$. After heat treatment, specimens were polished and etched with 3% nital solution for optical microscopy, scanning electron microscopy (SEM) and transmission electron microscopy (TEM). Specimens for TEM were machined from 3 mm diameter rods, which were sliced into $100\text{ }\mu\text{m}$ discs and ground

* Corresponding author. E-mail address: hkdb@cam.ac.uk

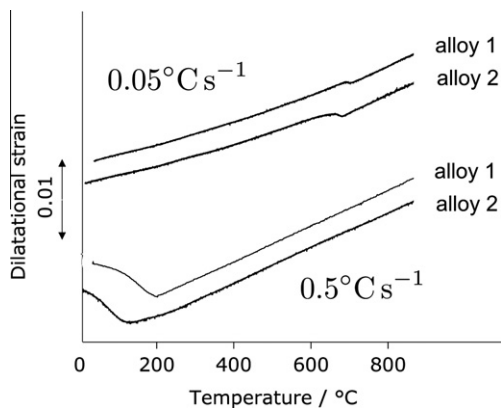
Table 1. Chemical compositions of the alloys studied (wt.%).

Alloy	C	Si	Mn	Mo	Cr	Co	Al	P	S	V	Ni
1	0.78	1.60	2.02	0.24	1.01	3.87	1.37	0.002	0.002	–	–
2	0.79	1.59	1.94	0.30	1.33	–	0.013	<0.002	–	0.11	0.02

down to 50 μm thickness using 1200 grit silicon carbide paper. The discs were then electropolished using a mixture of 5% perchloric acid, 15% glycerol and 80% methanol. The resulting foils were examined using a JEOL JEM-200CX transmission electron microscope operated at 200 kV.

Vickers hardness tests are reported as the average of at least 10 indentations made using a 1 kg load. Measurements of the interlamellar spacing of pearlite were performed using SEM and TEM images, with 10 fields studied for each case; the statistical uncertainties quoted refer to $\pm 1\sigma$. The true interlamellar spacing L was derived from the mean value \bar{S}_R of measurements on random sections according to $S = 0.5\bar{S}_R$ [9,10].

Typical measurements for Alloy 1 are illustrated in Figure 1, with pearlite forming over the temperature range 695–661 $^{\circ}\text{C}$ at a cooling rate of 0.05 $^{\circ}\text{C s}^{-1}$, with mostly martensite forming when the cooling rate is increased by a factor of 10. Further data are summarized in Table 2. Alloy 1 is able to transform into pearlite at

**Figure 1.** Dilatational strain as a function of temperature.

cooling rates below 0.1 $^{\circ}\text{C s}^{-1}$, whereas the corresponding rate for Alloy 2 has to be less than 0.05 $^{\circ}\text{C s}^{-1}$ and transformation is suppressed to lower temperatures when compared against the steel containing the cobalt and aluminium. As expected, both alloys were found to show increasing quantities of martensite at greater cooling rates. It should be noted that in these steels bainite requires too long to form during continuous cooling at the rates studied, which is why the residual phase after pearlitic transformation etches white relative to pearlite itself; optical micrographs for the two alloys cooled at 0.1 $^{\circ}\text{C s}^{-1}$ from the austenitization temperature are given in Figure 2.

Figure 3 shows typical scanning and transmission electron micrographs which reveal the extremely fine pearlite obtained, particularly in Alloy 1, when cooled at the slow rate of 0.02 $^{\circ}\text{C s}^{-1}$ in order to generate fully pearlitic microstructures. Quantitative measurements giving the true interlamellar spacing as a function of cooling rate are presented in Figure 4a, where the spacing is seen to be $S \approx 44\text{--}96\text{ nm}$ for Alloy 1 and $S \approx 80\text{--}128\text{ nm}$ for Alloy 2. A greater cooling rate leads to a finer spacing by suppressing the transformation to lower temperatures, but there is an upper limit to the cooling rate determined by incomplete transformation, as shown in Table 2.

Corresponding hardness data for just the fully pearlitic samples are shown in Figure 4b, where they are plotted as a function of S^{-1} [11]. It is interesting that all the data fall roughly on the same line, indicating that the major differences in the hardness of fully pearlitic samples is due to variations in interlamellar spacings. Note that the strength of pearlite is sometimes analysed in terms of a Hall–Petch relationship $S^{-1/2}$, but this is difficult to justify on the basis of the mechanism when considering undeformed, fine pearlite.

It has been demonstrated that the addition of cobalt and aluminium to a steel normally used to produce

Table 2. Data obtained from dilatometric experiments (pearlite and martensite are represented by the symbols P and α' , respectively).

Alloy	\dot{T} ($^{\circ}\text{C s}^{-1}$)	Start T ($^{\circ}\text{C}$)	Finish T ($^{\circ}\text{C}$)	Time interval (s)	Microstructure
Alloy 1	0.02	695	682	514	P
	0.05	694	680	438	P
	0.1	683	661	198	P
	0.5	197			$P + \alpha'$
	1	199			α'
	2	197			α'
Alloy 2	0.02	689	669	1100	P
	0.05	677	650	546	P
	0.1	662	639	235	$P + \alpha'$
	0.5	131			α'
	1	132			α'
	2	127			α'

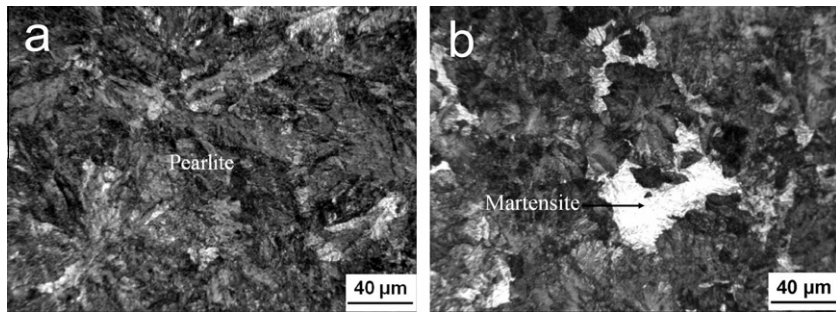


Figure 2. Optical micrographs of samples cooled at $0.1\text{ }^{\circ}\text{C s}^{-1}$. (a) Alloy 1; (b) Alloy 2.

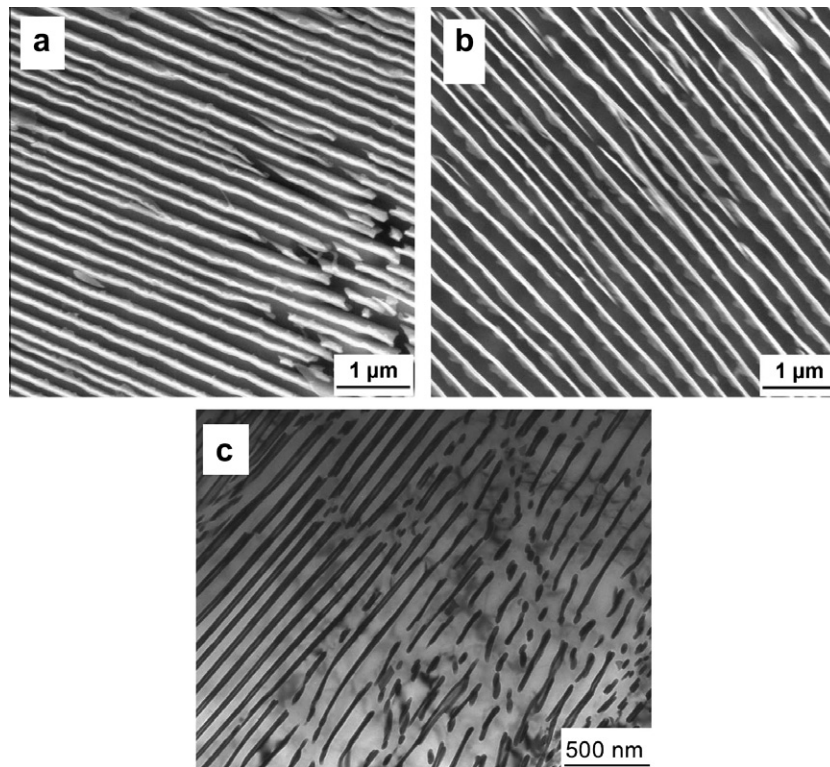


Figure 3. Samples cooled at $0.02\text{ }^{\circ}\text{C s}^{-1}$. (a) SEM image of Alloy 1; (b) SEM image of Alloy 2; (c) TEM image of Alloy 1.

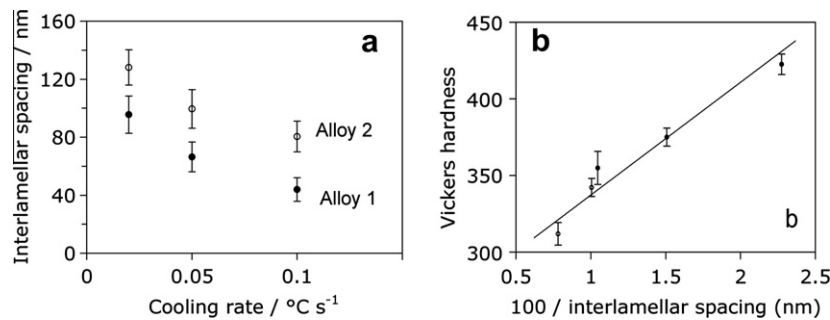


Figure 4. (a) Relationship between interlamellar spacing and cooling rate. (b) Hardness of fully pearlitic samples as a function of the inverse of the interlamellar spacing.

low-temperature bainite permits the alloy to transform completely into pearlite at slow cooling rates. This is because of the well-known effect of these solutes in enhancing the driving force for the transformation of

austenite into pearlite. The interlamellar spacing that can be obtained in this way can be as small as 50 nm (hardness 422 HV), which is somewhat finer than that transformed under the influence of a 30 T magnetic field.

Furthermore, the steel containing Co and Al is demonstrated to achieve finer interlamellar spacings even though it transforms at a higher temperature than the alloy free from these solutes. A comparison of the two alloys shows that the major differences in their hardnesses in the fully pearlitic state can be explained purely in terms of the variations in interlamellar spacing.

Further work is planned to understand the partitioning of solutes during the course of the austenite to pearlite transformation. This could be revealed by partial transformation into pearlite, followed by isothermal transformation at a lower temperature in order to preserve some austenite and the solute distribution at the austenite-pearlite interface.

K.M.W. gratefully acknowledges the financial support from the China Scholarship Council (CSC) and the State Ministry of Education (NCET-05-0680), and the invaluable assistance from colleagues at the University of Cambridge.

[1] F.G. Caballero, H.K.D.H. Bhadeshia, K.J.A. Mawella, D.G. Jones, P. Brown, *Mater. Sci. Technol.* 18 (2002) 279.

[2] H.K.D.H. Bhadeshia, *Proc. R. Soc. Lond. A* 466 (2010) 3.
 [3] R.A. Jaramillo, S.S. Babu, G.M. Ludtka, R.A. Kisner, J.B. Wilgen, G. Mackiewicz-Ludtka, D.M. Nicholson, S.M. Kelly, M. Muruganath, H.K.D.H. Bhadeshia, *Scripta Mater.* 52 (2004) 461.
 [4] R.A. Jaramillo, S.S. Babu, M.K. Miller, G.M. Ludtka, G. Mackiewicz-Ludtka, R.A. Kisner, J.B. Wilgen, H.K.D.H. Bhadeshia, in: J.M. Howe, D.E. Laughlin, J.K. Lee, U. Dahmen, W.A. Soffa (Eds.), *Solid-Solid Phase Transformations*, TME–AIME, Warrendale, PA, 2005, p. 873.
 [5] V.T.L. Buono, B.M. Gonzalez, T.M. Lima, M.S. Andrade, *J. Mater. Sci.* 32 (1997) 1005.
 [6] R.F. Mehl, W.C. Hagel, *Prog. Metal. Phys.* 6 (1956) 74.
 [7] H.I. Aaronson, H.A. Domian, G.M. Pound, *TMS–AIME* 236 (1966) 781.
 [8] C. Garcia-Mateo, F.G. Caballero, H.K.D.H. Bhadeshia, *ISIJ Int.* 43 (2003) 1821.
 [9] F.G. Caballero, C.G. de Andrés, C. Capdevila, *Mater. Charact.* 45 (2000) 111.
 [10] F.G. Caballero, C.G. de Andrés, C. Capdevila, *Scripta Mater.* 42 (2000) 537.
 [11] K.K. Ray, D. Mondal, *Acta Metall. Mater.* 39 (1991) 2201.